An Energy-Balance Model with Permafrost Feedback – Background

1 General

We consider a surface slab split into two components; ocean and land. The temperature of the ocean section is assumed to be uniform while the temperature of the land portion changes with depth. At the surface of both mediums their temperatures are equal, i.e. $T_O \equiv T_S(0, t)$ where T_O is the temperature of the ocean and $T_S(z, t)$ represents the temperature of the soil at time t and at depth $-Z_L \leq z \leq 0$. Land and ocean areas are assumed to be "well-mixed".

We assume fluxes within the soil section to be one-dimensional, acting normal to the surface-atmosphere interface. Applying energy conservation in the ocean layer and the modelling the heat equation in the soil yields

$$\rho_O c_O Z_O \frac{\partial T_S(0, t)}{\partial t} = -K_L \frac{\partial T_S(0, t)}{\partial z} + q(0, t) \tag{1}$$

$$\rho_L c_L \frac{\partial T_S(z, t)}{\partial t} = K_L \frac{\partial^2 T_S(z, t)}{\partial z^2} \tag{2}$$

$$T_S(-Z_L, t) = T_{Z_L} \tag{3}$$

where ρ is density in kg m^{-3}, c is specific heat capacity in J kg^{-1} K^{-1}, Z_O is the depth of our ocean slab in m, K_L the thermal conductivity of land in W m^{-1} K^{-1}, and q is the total flux source at the surface in W m^{-2}. Note that by equation (3) we impose the boundary condition that there exists a depth where temperature remains constant in the soil.

A simple energy balance to capture surface-atmosphere interactions and forcings can be seen below in Fig. 1.
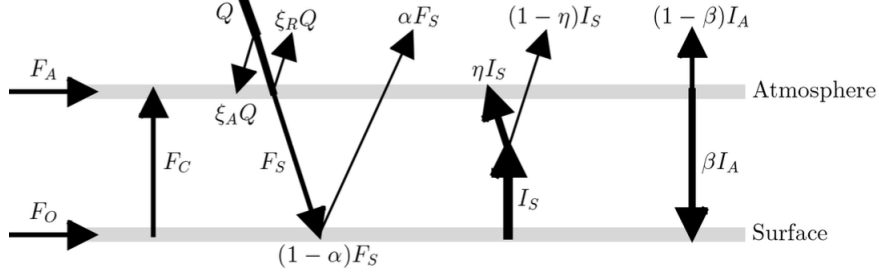
Figure 1: Pictorial representation of 2-slab EBM from Dortmans et al., 2019

Building on the EBM as outlined in Dortmans et al., 2019 (see the README) and interpreting terms in the figure above, the system of equations governing the climate model becomes

$$\rho_A c_A Z_A \frac{dT_A(t)}{dt} = F_A + F_C + \xi_A Q + \eta I_S - I_A$$

$$\rho_O c_O Z_O \frac{\partial T_S(0,t)}{\partial t} = -K_L \frac{\partial T_S(0,t)}{\partial z} + F_O - F_C + (1-\alpha)F_S - I_S + \beta I_A$$

$$\rho_L c_L \frac{\partial T_S(z,t)}{\partial t} = K_L \frac{\partial^2 T_S(z,t)}{\partial z^2}$$

$$T_S(-Z_L, t) = T_{Z_L}$$

We non-dimensionalize the above system using the following dimensionless variables

$$s = \frac{\sigma T_R^4}{c_O \rho_O Z_O T_R} t, \qquad \tau_S = \frac{T_S}{T_R}, \qquad \tau_A = \frac{T_A}{T_R}, \qquad \zeta = \frac{z}{Z_L},$$

where σ is the Stefan-Boltzmann constant and $T_R = 273.15K$ is our reference temperature. Here one unit of dimensionless time s corresponds to the amount of actual time required for the earth at T_R to radiate an equivalent amount of energy which is stored in our ocean slab at T_R.

The non-dimensional system becomes

$$H_1 \frac{d\tau_A(s)}{ds} = f_A + f_C + \xi_A q + \eta i_S - i_A \tag{4}$$

$$\frac{\partial \tau_S(0,s)}{\partial s} + H_2 \frac{\partial \tau_S(0,s)}{\partial \zeta} = f_O - f_C + (1-\alpha)f_S - i_S + \beta i_A \tag{5}$$

$$H_3 \frac{\partial \tau_S(\zeta,s)}{\partial s} = \frac{\partial^2 \tau_S(\zeta,s)}{\partial \zeta^2} \tag{6}$$

$$\tau_S(-1,s) = \tau_{Z_L} \tag{7}$$

where

$$H_1 = \frac{\rho_A c_A Z_A}{\rho_O c_O Z_O}, \qquad H_2 = \frac{K_L}{Z_L \sigma T_R^3}, \qquad H_3 = \frac{\rho_L c_L Z_L^2 \sigma T_R^3}{K_L \rho_O c_O Z_O}, \qquad \tau_{Z_L} = \frac{T_{Z_L}}{T_R},$$

$$f_A = \frac{F_A}{\sigma T_R^4}, \qquad f_C = \frac{F_C}{\sigma T_R^4}, \qquad f_O = \frac{F_O}{\sigma T_R^4}, \qquad q = \frac{Q}{\sigma T_R^4}, \qquad i_S = \frac{I_S}{\sigma T_R^4},$$

$$i_A = \frac{I_A}{\sigma T_R^4}$$

We are interested in equilibrium solutions to our system of equations where $\tau_S(\zeta, s) = \tau_S(\zeta)$ and $\tau_A(s) = \tau_A$. Our system thus becomes

$$0 = f_A + f_C + \xi_A q + \eta i_S - i_A \tag{8}$$

$$H_2 \frac{\partial \tau_S(0)}{\partial \zeta} = f_O - f_C + (1 - \alpha) f_S - i_S + \beta i_A \tag{9}$$

$$0 = \frac{\partial^2 \tau_S(\zeta)}{\partial \zeta^2} \tag{10}$$

$$\tau_S(-1) = \tau_{Z_L} \tag{11}$$

Solving this system we obtain

$$\tau_S(\zeta) = \tau_{Z_L} + \frac{\zeta + 1}{H_2} [f_O - (1 - \beta) f_C + (1 - \alpha) f_S - (1 - \beta \eta) i_S + \beta (f_A + \xi_A q)] \tag{12}$$

2 Permafrost

2.1 Background

Perennially frozen soils contain massive amounts of carbon which become increasingly susceptible to thaw as global temperatures rise. Carbon released from the permafrost contributes to atmospheric GHG burdens which in turn accelerates the warming process and results in further carbon losses from these soils. This is permafrost feedback.

In this permafrost module we limit our analysis to carbon stored within the top 3 m of High-Arctic permafrost soils, where the Arctic is defined as any region with latitude greater than or equal to 60° N. Carbon emission rates are determined from aerobic conditions, soil type and pool decomposition speed. We consider two soil types described by their organic carbon content; mineral soils which are <20%C by weight and organic soils which are ≥20%C by weight (Deimling et al., 2015). We use a 3-pool decomposition model where carbon falls into a passive, slow or active decomposition pool based on its lability. Carbon in the active pool is respired by permafrost soils within a year, carbon in the slow pool on a decadal scale, and carbon in the passive pool over hundreds

to thousands of years (Schädel et al., 2014). We assume carbon in the passive pool is inert.

In the simplest case, carbon is assumed to be respired from the permafrost in the form of CO_2 or CH_4. What determines this is the availability of oxygen in the decay process. It is assumed that aerobic decomposition produces strictly CO_2 while anaerobic decomposition produces CH_4. Of the carbon which decomposes anaerobically, a fraction is oxidized before reaching the surface-atmosphere interface. We assume this oxidized fraction is released as CO_2.

Both CO_2 and CH_4 are "well-mixed" within the atmosphere. The atmospheric lifetime of CH_4 is roughly a decade due to removal by the OH radical. We assume CH_4 is broken down into CO_2 during this process and that after 10 years the entirety of a CH_4 sample will have been converted to CO_2.

2.2 Decomposition

Suppose carbon is distributed within the soil according to some function $m(z,t)$. Using a temperature-dependent decay rate constant, $k(T)$, we express the decomposition of carbon at a specific depth in the soil as

$$\frac{dm(z,t)}{dt} = -k(T_S(z,t))m(z,t) \tag{13}$$

Let us denote by $m_O(z,t)$ the mass distribution of carbon in pools where aerobic decomposition takes place, $m_X(z,t)$ the mass distribution of carbon in anaerobic pools where oxidation occurs, and $m_N(z,t)$ the mass distribution of carbon in anaerobic pools with no oxidation. These pools decompose according to equation (13) with their own decay rate constants. We then express the decay of permafrost carbon into CO_2 and CH_4 as follows

$$\frac{dCO_2(t)}{dt} = \frac{M_{CO_2}}{M_C} \int_{Z_L}^0 k_O(T_S(z,t))m_O(z,t) + k_X(T_S(z,t))m_X(z,t)dz \tag{14}$$

$$\frac{dCH_4(t)}{dt} = \frac{M_{CH_4}}{M_C} \int_{Z_L}^0 k_N(T_S(z,t))m_N(z,t)dz \tag{15}$$

Here M_C, M_{CO_2} and M_{CH_4} are the molar masses of C, CO_2 and CH_4. Equations (14) and (15) describe release rates of each gas. One should note that since we've assumed carbon is only in the top 3 m, the lower bound on the integrals above can be replaced with -3.

Once in the atmosphere we must consider sink terms introduced by the OH radical which acts to remove CH_4 and convert it to CO_2 (by assumption). Modifying

the above equations we obtain

$$\frac{dCO_2(t)}{dt} = \frac{M_{CO_2}}{M_C} \int_{Z_L}^0 k_O(T_S(z,t))m_O(z,t) + k_X(T_S(z,t))m_X(z,t)dz$$

$$+(\frac{M_{CO_2}}{M_{CH_4}})r_{CH_4}CH_4(t) \tag{16}$$

$$\frac{dCH_4(t)}{dt} = \frac{M_{CH_4}}{M_C} \int_{Z_L}^0 k_N(T_S(z,t))m_N(z,t)dz - r_{CH_4}CH_4(t) \tag{17}$$

where r_{CH_4} is the decay rate constant for the removal of CH_4 by OH.

3   Modelling

We first construct a discrete version our mass distribution function by partitioning the top 3 m of our surface slab into P pools and dividing the total permafrost carbon amongst them. Denote by $m^i(t) = m(z^i, t)$ the mass distribution of carbon in pool i with $z^i = -3(\frac{i-1}{P})$. Likewise, define by $T^i(t) = T(z^i, t)$ the temperature of the ith pool.

In order to determine the effect of permafrost feedback on the EBM, we need solutions to equations (16) and (17) which in turn requires knowledge of $m(z, t)$. In the discrete case, the system of equations governing this problem becomes

$$\frac{dm^i(t)}{dt} = -k_O(T_S^i(t))m_O^i(t) - k_X(T_S^i(t))m_X^i(t) - k_N(T_S^i(t))m_N^i(t)$$

$$\frac{dCO_2(t)}{dt} = \frac{M_{CO_2}}{M_C} \sum_{i=1}^P k_O(T_S^i(t))m_O^i(t) + k_X(T_S^i(t))m_X^i(t) + (\frac{M_{CO_2}}{M_{CH_4}})r_{CH_4}CH_4(t)$$

$$\frac{dCH_4(t)}{dt} = \frac{M_{CH_4}}{M_C} \sum_{i=1}^P k_N(T_S^i(t))m_N^i(t) - r_{CH_4}CH_4(t)$$

$$\tag{18}$$

The solution to this system of $P+2$ differential equations is a function $u(t)$ such that

$$\dot{u}(t) = \begin{bmatrix} \frac{m^1(t)}{dt} \\ \frac{m^2(t)}{dt} \\ \vdots \\ \frac{m^P(t)}{dt} \\ \frac{dCO_2(t)}{dt} \\ \frac{dCH_4(t)}{dt} \end{bmatrix}, \ u(t_0) = \begin{bmatrix} m^1(t_0) \\ m^2(t_0) \\ \vdots \\ m^P(t_0) \\ 0 \\ 0 \end{bmatrix}$$

Here we assume that no permafrost carbon is present in the atmosphere in the

year t_0. We numerically solve for $u(t)$ using a Adams-Bashforth 3-step method along different RCP projections with $u(t_1)$ and $u(t_2)$ being obtained from a third order Runge-Kutta method.

System (18) allows us to model permafrost contributions to the global atmospheric budgets of CO_2 and CH_4 given the temperature of our surface slab. As such we need a means of determining $T_S(t)$ if we wish to model Arctic temperatures over time. We accomplish this using Representative Concentration Pathways (RCPs) as provided by the Intergovernmental Panel on Climate Change which projects atmospheric concentrations for GHG's from anthropogenic sources until the year 2500.

We neatly describe the total atmospheric concentrations of CO_2 and CH_4 on a yearly basis as a sum of anthropogenic (RCP) and permafrost sources. These terms appear in the calculation of absorptivity (η) in equation (12) which in turn is used to calculate $T_S(t)$. For more information see Dortmans et al., 2019.

4 Supplementary

4.1 Physical parameters

Symbol	Description	Value	Reference
C_{tot}	Total C stocks	1300 PgC	Hugelius et al., 2014
S_A	Surface area of Arctic region	3.42×10^{13} m^2	N/A
S_P	Permafrost surface area	1.78×10^{13} m^2	Hugelius et al., 2014
Z_L	Soil slab depth	15 m	Biskaborn et al., 2018
$T_S(-Z_L, t)$	Constant temperature at bottom of surface slab	-3.054°C	Biskaborn et al., 2018
K_L	Thermal conductivity of Arctic soils	2 W m^{-1} K^{-1}	Rasmussen et al., 2018
$\gamma_{a,ms}$	Fraction of carbon available for decomposition in active pool, mineral soils	0.013	Schädel et al., 2014
$\gamma_{s,ms}$	Fraction of carbon available for decomposition in slow pool, mineral soils	0.107	Schädel et al., 2014
$\gamma_{a,o}$	Fraction of carbon available for decomposition in active pool, organic soils	0.015	Schädel et al., 2014
$\gamma_{s,o}$	Fraction of carbon available for decomposition in slow pool, organic soils	0.293	Schädel et al., 2014
f_{ms}	Mass fraction of carbon in mineral soils	0.708	Hugelius et al., 2014

f_o	Mass fraction of carbon in organic soils	0.292	Hugelius et al., 2014
$A_{ms,an}$	Area fraction of mineral soil with anaerobic decomposition	0.05	Deimling et al., 2012
$A_{o,an}$	Area fraction of organic soils with anaerobic decomposition	0.8	Frolking et al., 2001
χ_{ms}	Fraction of CH_4 oxidized in mineral soils	0.25	Deimling et al., 2012
χ_o	Fraction of CH_4 oxidized in organic soils	0.6	Deimling et al., 2012
$R_{an/a}$	Ratio of decomposition rates in aerobic and anaerobic conditions	0.1	Deimling et al., 2012
Q_{10}	Q_{10} temperature sensitivity	2.5	Schädel et al., 2014
$\kappa_{a,ms}$	Active pool decomposition rate constant at 5 °C in mineral soils under aerobic conditions	2.8986	Schädel et al., 2014
$\kappa_{s,ms}$	Slow pool decomposition rate constant at 5 °C in mineral soils under aerobic conditions	0.1318	Schädel et al., 2014
$\kappa_{a,o}$	Active pool decomposition rate constant at 5 °C in organic soils under aerobic conditions	2.4390	Schädel et al., 2014
$\kappa_{s,o}$	Slow pool decomposition rate constant at 5 °C in organic soils under aerobic conditions	0.1387	Schädel et al., 2014
r_{CH_4}	Atmospheric decay rate of CH_4	0.0762	N/A

Table 1: Constants used in permafrost module

4.2 Derivation of $\dot{m}_O$, $\dot{m}_X$, and $\dot{m}_N$

Suppose the carbon mass distribution in permafrost soils is given by $m(z,t)$. We assume carbon pools corresponding to anaerobic, anaerobic with oxidation and anaerobic without oxidation are well-mixed such that the mass of carbon in each pool can be expressed in the form fraction times $m(z,t)$. Our goal is to construct these fractions.

Using assumptions outlined in section 2.1 as well as parameters listed in Table 1 we arrive at

$$m_O(z,t) = m(z,t)(f_{ms}(1 - A_{ms,an}) + f_o(1 - A_{o,an})) \tag{19}$$

$$m_X(z,t) = m(z,t)(f_{ms}A_{ms,an}\chi_{ms} + f_oA_{o,an}\chi_o) \tag{20}$$

$$m_N(z,t) = m(z,t)(f_{ms}A_{ms,an}(1 - \chi_{ms}) + f_oA_{o,an}(1 - \chi_o)) \qquad (21)$$

Now by equation (13) all we need to convert the above equations into emission rates is the introduction of a decomposition rate constant, k. We express this value as a sum of active pool and slow pool contributions in mineral and organic soils.

$$\begin{aligned}
\frac{dm_O(z,t)}{dt} = -m(z,t)(f_{ms}(1 - A_{ms,an})[\gamma_{a,ms}k_{a,ms}(T_S(z,t)) \\
+\gamma_{s,ms}k_{s,ms}(T_S(z,t))] + f_o(1 - A_{o,an})[\gamma_{a,o}k_{a,o}(T_S(z,t)) \\
+\gamma_{s,o}k_{s,o}(T_S(z,t))])
\end{aligned} \qquad (22)$$

$$\begin{aligned}
\frac{dm_X(z,t)}{dt} = -m(z,t)(f_{ms}A_{ms,an}\chi_{ms}[\gamma_{a,ms}R_{an/a}k_{a,ms}(T_S(z,t)) \\
+\gamma_{s,ms}R_{an/a}k_{s,ms}(T_S(z,t))] + f_oA_{o,an}\chi_o[\gamma_{a,o}R_{an/a}k_{a,o}(T_S(z,t)) \\
+\gamma_{s,o}R_{an/a}k_{s,o}(T_S(z,t))])
\end{aligned} \qquad (23)$$

$$\begin{aligned}
\frac{dm_N(z,t)}{dt} = -m(z,t)(f_{ms}A_{ms,an}(1 - \chi_{ms})[\gamma_{a,ms}R_{an/a}k_{a,ms}(T_S(z,t)) \\
+\gamma_{s,ms}R_{an/a}k_{s,ms}(T_S(z,t))] + f_oA_{o,an}(1 - \chi_o)[\gamma_{a,o}R_{an/a}k_{a,o}(T_S(z,t)) \\
+\gamma_{s,o}R_{an/a}k_{s,o}(T_S(z,t))])
\end{aligned} \qquad (24)$$

here $k(T_S(z,t))$ is an annual effective decomposition rate given by

$$k(T_S(z,t)) = \frac{1}{2\pi}\int_0^{2\pi} g(T,t)dt \qquad (25)$$

where

$$g(T,t) = \begin{cases} \kappa \cdot Q_{10}^{\frac{T_S(z,t)-5}{10}} & T + \Delta T \sin t > 0 \\ 0 & else \end{cases} \qquad (26)$$

With equations (25) and (26) we capture the effects of seasonal temperature fluctuations so that even when the annual mean temperature is below freezing there can still be permafrost thaw as a consequence of higher temperatures experienced in the spring and summer months.

By substituting equations (22) through (24) into equations (16) and (17) we are able to describe the emission rates of CO_2 and CH_4.

References

Biskaborn, B. K., Smith, S. L., Noetzli, J., Matthes, H., Vieira, G., Streletskiy, D. A., Schoeneich, P., Romanovsky, V. E., Lewkowicz, A. G., Abramov, A., Allard, M., Boike, J., Cable, W. L., Christiansen, H. H., Delaloye, R., Diekmann, B., Drozdov, D. S., Etzelmüller, B., Grosse, G., ... Lantuit, H. (2018). *GTN-P global mean annual ground temperature data for permafrost near the depth of zero annual amplitude (2007-2016)* (tech. rep.). https://doi.org/10.1038/s41467-018-08240-4

Deimling, T. S. V., Grosse, G., Strauss, J., Schirrmeister, L., Morgenstern, A., Schaphoff, S., Meinshausen, M., & Boike, J. (2015). Observation-based modelling of permafrost carbon fluxes with accounting for deep carbon deposits and thermokarst activity. *Biogeosciences*, *12*, 3469.

Deimling, T. S. V., Meinshausen, M., Levermann, A., Huber, V., Frieler, K., Lawrence, D., & Brovkin, V. (2012). Estimating the near-surface permafrost-carbon feedback on global warming. *Biogeosciences*, *9*, 649.

Dortmans, B., Langford, W. F., & Willms, A. R. (2019). An energy balance model for paleoclimate transitions. *Climate of the Past*, *15*(2), 493–520. https://doi.org/10.5194/cp-15-493-2019

Frolking, S., Roulet, N. T., Moore, T. R., Richard, P. J. H., Lavoie, M., & Muller, S. D. (2001). Modeling Northern Peatland Decomposition and Peat Accumulation. *Ecosystems*, *4*, 479–498.

Hugelius, G., Strauss, J., Zubrzycki, S., Harden, J., Schuur, E. A. G., Ping, C.-L., Schirrmeister, L., Grosse, G., Michaelson, G., Koven, C., O'Donnell, J., Elberling, B., Mishra, U., Camill, P., Yu, Z., Palmtag, J., & Kuhry, P. (2014). Estimated stocks of circumpolar permafrost carbon with quantified uncertainty ranges and identified data gaps. *Biogeosciences*, *11*, 6573.

Rasmussen, L. H., Zhang, W., Hollesen, J., Cable, S., Christiansen, H. H., Jansson, P.-E., & Elberling, B. (2018). Modelling present and future permafrost thermal regimes in northeast greenland. *Cold Regions Science and Technology*, *146*, 199–213. https://doi.org/https://doi.org/10.1016/j.coldregions.2017.10.011

Schädel, C., Schuur, E. A. G., Bracho, R., Elberling, B., Knoblauch, C., Lee, H., Luo, Y., Shaver, G. R., & Turetsky, M. R. (2014). Circumpolar assessment of permafrost C quality and its vulnerability over time using long-term incubation data. *Global Change Biology*, *20*, 641–652.